



Commercial off-the-Shelf (COTS) Refractory Material Evaluation

Luz Marina Calle
NASA, Kennedy Space Center

Mark R. Kolody
ASRC, Aerospace Corporation

Jerome P. Curran
ASRC, Aerospace Corporation

Teddy Back
ASRC, Kennedy Space Center

Paul E. Hintze
NASA, Kennedy Space Center

Christopher R. Parlier
NASA, Kennedy Space Center

Jeffrey W. Sampson
NASA, Kennedy Space Center

Stephen Perusich
ASRC, Kennedy Space Center

Cori Bucherl
NASA, Kennedy Space Center

NASA STI Program...in Profile

Since its founding, NASA has been dedicated to the advancement of aeronautics and space science. The NASA Scientific and Technical Information (STI) program plays a key part in helping NASA maintain this important role.

The NASA STI Program operates under the auspices of the Agency Chief Information Officer. It collects, organizes, provides for archiving, and disseminates NASA's STI. The NASA STI program provides access to the NASA Aeronautics and Space Database and its public interface, the NASA Technical Reports Server, thus providing one of the largest collections of aeronautical and space science STI in the world. Results are published in both non-NASA channels and by NASA in the NASA STI Report Series, which includes the following report types:

- **TECHNICAL PUBLICATION.** Reports of completed research or a major significant phase of research that present the results of NASA programs and include extensive data or theoretical analysis. Includes compilations of significant scientific and technical data and information deemed to be of continuing reference value. NASA counterpart of peer-reviewed formal professional papers but has less stringent limitations on manuscript length and extent of graphic presentations.
- **TECHNICAL MEMORANDUM.** Scientific and technical findings that are preliminary or of specialized interest, e.g., quick release reports, working papers, and bibliographies that contain minimal annotation. Does not contain extensive analysis.
- **CONTRACTOR REPORT.** Scientific and technical findings by NASA-sponsored contractors and grantees.
- **CONFERENCE PUBLICATION.** Collected papers from scientific and technical conferences, symposia, seminars, or other meetings sponsored or cosponsored by NASA.
- **SPECIAL PUBLICATIONS.** Scientific, technical, or historical information from NASA programs, projects, and missions, often concerned with subjects having substantial public interest.
- **TECHNICAL TRANSLATION.** English-language translations of foreign scientific and technical material pertinent to NASA's mission.

Specialized services also include creating custom thesauri, building customized databases, organizing and publishing research results.

For more information about the NASA STI program, see the following:

- Access the NASA STI program home page at <http://www.sti.nasa.gov>
- E-mail your question via the Internet to help@sti.nasa.gov
- Fax your question to the NASA STI Help Desk at 443-757-5803
- Telephone the NASA STI Help Desk at 443-757-5802
- Write to:
NASA Center for AeroSpace Information (CASI)
7115 Standard Drive
Hanover, MD 21076-1320

NASA/TM-2013-216317



Commercial off-the-Shelf (COTS) Refractory Material Evaluation

Luz Marina Calle
NASA, Kennedy Space Center

Mark R. Kolody
ASRC, Aerospace Corporation

Jerome P. Curran
ASRC, Aerospace Corporation

Teddy Back
ASRC, Kennedy Space Center

Paul E. Hintze
NASA, Kennedy Space Center

Christopher R. Parlier
NASA, Kennedy Space Center

Jeffrey W. Sampson
NASA, Kennedy Space Center

Stephen Perusich
ASRC, Kennedy Space Center

Cori Bucherl
NASA, Kennedy Space Center

**National Aeronautics and
Space Administration**

Kennedy Space Center

December 9, 2009

Available from:

NASA Center for AeroSpace Information
7115 Standard Drive
Hanover, MD 21076-1320

National Technical Information Service
5301 Shawnee Road
Alexandria, VA 22312

Available in electronic form at <http://www.sti.nasa.gov>.

Executive Summary

Fondu Fyre (FF) is currently the only refractory material qualified for use in the flame trench at KSC's Shuttle Launch Pads 39A and 39B. However, the material is not used as it was qualified and has undergone increasingly frequent and severe degradation due to the launch blasts. This degradation is costly as well as dangerous for launch infrastructure, crew and vehicle. FF is applied at the pad via the gunnite process, where wetted refractory material is sprayed onto a steel grid mounted on a support structure. The water content in this process can be manually adjusted by operators, causing distinct visual and physical discrepancies among repair areas. Since the application process is unlikely to change for new refractory materials, it is important to understand the effects of water content on commercial off-the-shelf (COTS) refractory materials. The purpose of this study was to evaluate the performance of the FF with respect to various water contents as well as heat treatments, to simulate aging and exposure to the blast. Initial results indicated that different water contents and heat treatments result in distinct differences in crushing strength, apparent porosity and bulk density. However, water content became an insignificant factor in both crush strength and porosity when FF was cured to at least 1500°F. Additionally, inspection of the material's surface microstructure by scanning electron microscopy indicated distinguishable characteristics for different heat treatment levels. Results from this study will help guide future studies on the development and identification of new refractory materials.

This page intentionally left blank.

Contents

1	INTRODUCTION	1
2	EXPERIMENTAL APPROACH.....	3
3	EXPERIMENTAL PROCEDURES	4
3.1	Casting	4
3.2	Heat Treatment.....	4
3.3	Cold Crushing Strength Testing.....	5
3.4	Porosity Testing	5
3.5	SEM Sample Preparation.....	5
3.6	Statistical Analysis.....	6
4	RESULTS	6
4.1	Visual Changes	6
4.2	Crushing Strength	6
4.3	Porosity and Bulk Density	8
4.4	SEM Analysis	11
5	CONCLUSIONS.....	12
6	REFERENCES	12
APPENDIX A.	MINITAB OUTPUTS	13
APPENDIX B.	ADDITIONAL SEM IMAGES	17
APPENDIX C.	SPECIAL MIXING/USING INSTRUCTION FONDU FYRE® WA-1	19
APPENDIX D.	CRUSHING STRENGTH DATA [8]	21
APPENDIX E.	DATA USED TO CALCULATE POROSITY AND BULK DENSITY ACCORDING TO ASTM C20.....	23

Figures

Figure 1.	Flame trench wall repairs at Pad 39A.....	1
Figure 2.	FF crush strengths normal to striations	2
Figure 3.	MINITAB Output: One-way ANOVA: Crush strength (psi) versus Shift.....	2
Figure 4.	Five-Quart Hobart Mixer.....	4
Figure 5.	Crushed test specimen after failure	4
Figure 6.	Suspended weight apparatus for porosity measurement	5
Figure 7.	Array of heat-treated FF specimens (100% water content).....	6
Figure 8.	Crush strength results FF: Various water compositions and heat treatments.....	7
Figure 9.	Minitab output: One-way ANOVA: Crush strength (psi) versus heat Trt (°F).....	8

Figure 10. Comparison of crushing strength between gunned specimens [3] and cast specimens prepared in this study8

Figure 11. Apparent porosity of FF with different water contents and heat treatments9

Figure 12. Bulk density of FF with different water contents and heat treatments10

Figure 13. Minitab output: One-way ANOVA: Apparent Porosity versus Heat Treatment (°F)10

Figure 14. From top to bottom, 5000x SEM images of 100% FF treated at 2000°F, 1000°F, and 75°F11

Figure 15. One-way ANOVA: 75°F Crush strength versus Water Composition13

Figure 16. One-way ANOVA: 500°F Crush strength versus Water Composition13

Figure 17. One-way ANOVA: 1000°F Crush strength versus Water Composition13

Figure 18. One-way ANOVA: 1500°F Crush strength versus Water Composition14

Figure 19. One-way ANOVA: 2000°F Crush strength versus Water Composition14

Figure 20. One-way ANOVA: 75°F Porosity versus Water Composition14

Figure 21. One-way ANOVA: 500°F Porosity versus Water Composition15

Figure 22. One-way ANOVA: 1000°F Porosity versus Water Composition15

Figure 23. One-way ANOVA: 1500°F Porosity versus Water Composition15

Figure 24. One-way ANOVA: 2000°F Porosity versus Water Composition16

Figure 25. From top to bottom: 5000x SEM images of 1000°F heat treatment for 90%, 100%, and 110% water content FF17

Figure 26. From top to bottom: 5000x SEM images of 2000°F heat treatment for 90%, 100%, and 110% water content FF17

Figure 27. From top to bottom: 5000x SEM images of 75°F heat treatment for 90%, 100%, and 110% water content FF18

Figure 28. From top to bottom: SEM images of 90% water content heat treated to 1000°F, 1000°F and 75°F18

Tables

Table 1. Number of samples for each water composition and heat treatment3

Table 2. Comparison of apparent porosity and bulk density of cast samples and historic samples from SSME flame deflector10

Acronyms and Symbols

°C	degree Celsius
°F	degree Fahrenheit
COTS	Commercial off-the-Shelf
ETDP	Exploration Technology Development Program
FF	Fondu Fyre
FOD	Foreign Object Debris
KSC	Kennedy Space Center
LC	Launch Complex
NASA	National Aeronautics and Space Administration
SEM	Scanning Electron Microscope
CAC	Calcium Aluminate Cement
SSME	Space Shuttle Main Engine

This page intentionally left blank.

1 INTRODUCTION

Fondu Fyre (FF) is currently the only refractory material qualified for flame trench protection at KSC's Launch Complex 39. It has been in use since 1966, when it was determined to be the "best all around coating for large-scale applications." [1] However, the material does not meet qualification requirements of the NASA specification because it is not used at the pad as it was qualified [2]. Conventional refractory products (based on calcium aluminate cement) are generally cured, dried, and sintered (heated) to maximize their performance. Regardless of general practices, FF used at the KSC launch pad for protection of the flame deflector steel structure is not cured, dried, or sintered after application on the flame deflector surface. Corrosion degradation of the refractory material has resulted in increasingly frequent failures and liberation of material, jeopardizing the safety of the launch complex, crew, and vehicle and compromising the underlying steel structure integrity of the flame trench. This poor performance and degradation requires costly and extensive repairs, and is currently without a long term solution, looking forward into the Constellation Program.

FF application at Pad 39A entails a process called gunniting in which an operator manually directs (i.e., sprays) pressurized and wetted refractory material into a steel grid frame welded to the flame trench wall. Operators may subjectively alter the amount of water added during the gunnite process in order to achieve successful adhesion of the refractory to the grid structure. This opportunity for subjective application has led to obvious visual discrepancies among panels sprayed by different operators, as can be seen by the checkered pattern on the flame trench wall in Figure 1.



Figure 1. Flame trench wall repairs at Pad 39A

A September 2008 study [3]¹ by NASA Malfunction Analysis team measured the cold compression strength of four different gunnited FF samples. Two different operators gunned four total samples, one each at the beginning and end of their respective shifts. At least 10 compression tests were completed for each FF sample, the raw data for which are summarized numerically in the Malfunction Analysis report and graphically in Figure 2 below. A statistical analysis of the raw data (see Figure 3 below) indicates a significant difference of crushing strengths both between the two operators and between the start- and end- of shift gunning of a single operator. Compression strengths were measured for FF specimens (in the shape of a cube) at two different orientations, based on the striations that occur in the material due to gunnite operation. The striations form because the material is applied in thin layers until the desired thickness is achieved. NASA Malfunction Analysis team decided to investigate the effect of the striations on compressive strength by loading half of the specimens parallel to the striations and half normal to striations.

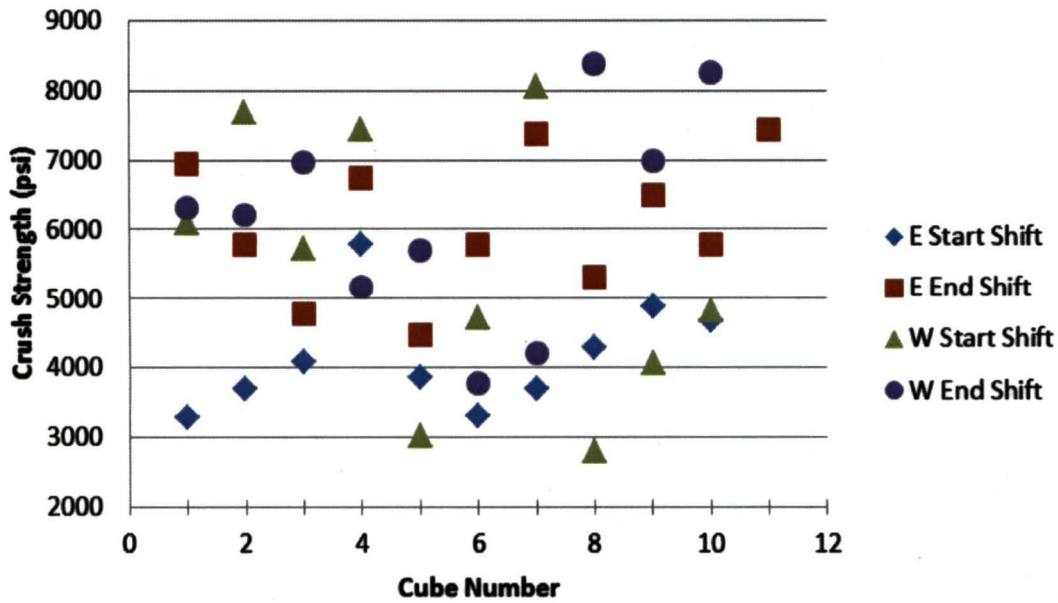


Figure 2. FF crush strengths normal to striations

The Minitab results are summarized in Figure 3 below. Statistical differences between means are indicated when the standard deviations do not overlap. The statistical results indicated that the normal-to-striations crushing strengths of the samples gunned by the East Wall Operator (E Start Shift, E End Shift) are significantly different, despite being gunned by the same person. The West Wall Operator’s samples (W Start Shift, W End Shift) do not display statistical differences. The difference, however, between East Operator’s Start-of-Shift sample and West Operator’s End-of-Shift sample is statistically significant.

Statistical analysis of the crush strength results for the parallel-to-striations loaded cubes displayed no significant difference of performance among sample sets.

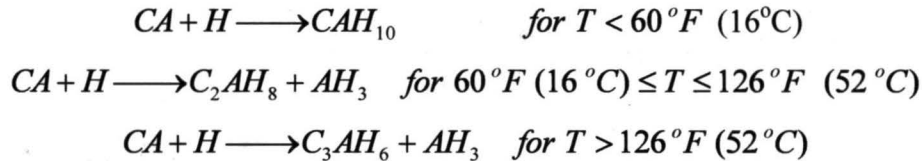
Individual 95% CIs For Mean Based on Pooled StDev				
Level	N	Mean	StDev	
E Start Shift	10	4160	780	(-----*-----)
E End Shift	11	6084	1001	(-----*-----)
W Start Shift	10	5443	1887	(-----*-----)
W End Shift	10	6195	1543	(-----*-----)

4000 5000 6000 7000

Figure 3. MINITAB Output: One-way ANOVA: Crush strength (psi) versus Shift

These discrepancies cannot be attributed to anything more objective than the relative times at which the samples were gunned and by which operators. The purpose of this study, therefore, is to reproducibly evaluate the effect of water content, as well as heat treatments, on the physical properties of FF. Outcomes from this study will enable an objective determination for the effect of operator water-addition inconsistencies on FF performance at Pad 39A.

Heat treatment was chosen as a parameter in these tests for two reasons: it accelerates the dehydration process that occurs during aging of the refractory material, and to determine how water content during application might affect the performance during a launch. Heat treatment of a calcium aluminate cement (CAC), such as FF, results in changes in the degree of hydration of the calcium aluminate phases. These reactions depend on the temperature. Some of the reactions are as follows:



Where C is calcium oxide (CaO), A is alumina (Al₂O₃), and H is water (H₂O). Heating above the temperatures of these reactions eventually leads to non-hydrated CA₆. Because the CAH₁₀ and the C₂AH₈ are metastable, over extended periods or when the CAC concrete is exposed to heat, these phases will convert to C₃AH₆. This conversion results in a 52.5% and 33.7% volume reduction for the CAH₁₀ and C₂AH₈, respectively. If this conversion occurs after the concrete has set, the porosity of the CAC concrete increases significantly and the strength decreases.

2 EXPERIMENTAL APPROACH

The experimental matrix in Table 1 was used to obtain behavioral trends of FF with respect to water content and temperature.

Table 1. Number of samples for each water composition and heat treatment

Heat Treatment Temperature (°F)	Water Composition (% of manufacturer-recommended value)		
	90	100	110
ambient (~75)	10	10	10
500	10	10	10
1000	10	10	10
1500	10	10	10
2000	10	10	10

The specimens evaluated in this study were cast in a laboratory in order to maintain control over the systemic water content. Two measurements were obtained from each condition (five specimens per test): cold crushing strength and apparent porosity, using ASTM C133 [4] and ASTM C20 [5], respectively. The specimen casting was performed using ASTM C862 [6] with some modifications, based on manufacturer recommendations [7]. The manufacturer-recommended a water content for FF of 14% by weight or 0.98 kg water to 7.0 kg FF [7]. The 90% and 110% manufacturer-recommended water content corresponded to 0.88 and 1.1 kg water to 7 kg FF, respectively.

3 EXPERIMENTAL PROCEDURES

3.1 Casting

The casting procedure followed ASTM 862 [6], the Pryor Giggey Special Mixing/Using Instructions [7], and original steps taken to achieve consistent cast specimens. Pryor-Giggey recommends 14.0% water by weight for mixing FF. Three different batches were prepared, one each for 100%, 90%, and 110% of the recommended water content. For each batch, water and dry FF were weighed into appropriate proportions for addition to the Five-Quart Hobart Mixer (Figure 4) recommended by ASTM 862. FF dry weight never exceeded 18.7 lb (8.5 kg) in order to allow adequate space in the mixer for the paddle to begin rotation. Per ASTM 862, the mixer was on low while the water addition was completed within one minute. A modification to the Test Standard included mixing on high (level 2) for 3 minutes following the water addition. Mixing at a lower speed than that did not achieve acceptable mixing. As quickly as possible following the mixing phase, the wet FF was packed into 2-in cubes or 2-in by 2-in by 11-in bricks. The FF in the molds was consolidated using a vibration table until the top surfaces appeared smooth; material was added or removed as necessary. The filled molds were placed in a humidity chamber (greater than 95% humidity) at ambient temperature for a curing period of 24 hours, after which the specimens were removed from the molds and allowed to continue curing at ambient conditions for at least seven days prior to the commencement of property measurements. The large bricks were cut to size with a diamond blade cutoff saw.



Figure 4. Five-Quart Hobart Mixer

3.2 Heat Treatment



Figure 5. Crushed test specimen after failure

Heat treatments were completed in either a Vulcan 3-550 or a Carbolite CWF 1300 furnace. The temperature ramping rate for each treatment was set at 104°F/min (40°C/min). Each treatment lasted 24 hours, after which the oven temperature was allowed to reach 230°F (110°C), at which temperature the specimens could remain dry until property testing.

3.3 Cold Crushing Strength Testing

Cold crushing strengths were determined using an Instron 5889 Universal Testing Machine with a loading rate of 7000 lbf/min. The dimensions of each specimen were measured per ASTM C133 [4]. Instron Bluehill Software was used to record all corresponding strength data. Following failure, each specimen was photographed (Figure 5), labeled and bagged for potential future evaluation.

3.4 Porosity Testing



Figure 6. Suspended weight apparatus for porosity measurement

Porosity testing was performed per ASTM C20 [5]. Each cube was dried at 230°F and weighed to get a dry mass. The samples were then held for 2 hours in boiling water. Following the boiling step, specimens were soaked in water for at least 24 hours at ambient temperatures. The saturated specimens were then weighed in air and in water, to obtain the saturated mass and suspended mass, respectively. Saturated mass was obtained using a traditional digital scale. To obtain suspended mass, a stand with a horizontally attached bar and a wire basket hanging from one end was placed on a scale. A 2 L beaker was filled with water and placed underneath the wire basket. With the basket in the water, the scale was tared. Suspended mass measurements were recorded as the mass of a specimen freely hanging in the wire basket (not touching the walls of the beaker) and completely submerged in water. Figure 6 shows a specimen in the process of a suspended mass measurement. All weight measurements were recorded and utilized per the calculation procedure in ASTM C20 to obtain apparent porosity values. Other properties attainable from ASTM C20 for the same measurements include exterior volume, volumes of open pores and impervious portions, water absorption, apparent specific gravity, and bulk density.

3.5 SEM Sample Preparation

In order to complete an SEM analysis of concrete specimens, small pieces from the larger cubes had to be liberated and either mounted as small pieces (approximately 3 mm × 5 mm × 2 mm) or ground into powder and mounted as such. Each fractured or powdered specimen was mounted on SEM sample stubs using carbon tape. The solid pieces were coated around the edges with carbon

paint and all specimens were coated with gold to increase electrical conduction. SEM images were taken with a JEOL 7500F Field Emission SEM.

3.6 Statistical Analysis

Statistical analysis was carried out using Minitab 15 (Minitab Inc.). One-way or two-way ANOVA was performed to determine if heat or water content treatments had a statistically significant effect on the physical properties of the FF. All analyses were performed at a 95% confidence level. When significant effects were identified, a Tukey pairwise comparison was performed to identify which means were significantly different from each other. Statistical differences between means are indicated when the standard deviations do not overlap.

4 RESULTS

4.1 Visual Changes

Visual changes were immediately apparent following the completion of heat treatments, as can be seen in Figure 8. Ambient cured samples were a dull grey color. As the heat treatment temperature increased, the color changed to a more reddish color. At 1000°F heat treatment, the color was similar to the color of an archived specimen that had been cut from the SSME flame trench. At higher heating temperatures, the samples changed to a lighter color. There was no color differences between the samples prepared with different water contents. The samples prepared with 90% recommended water did not flow as well during casting, and this was apparent in that the samples appeared less consolidated.

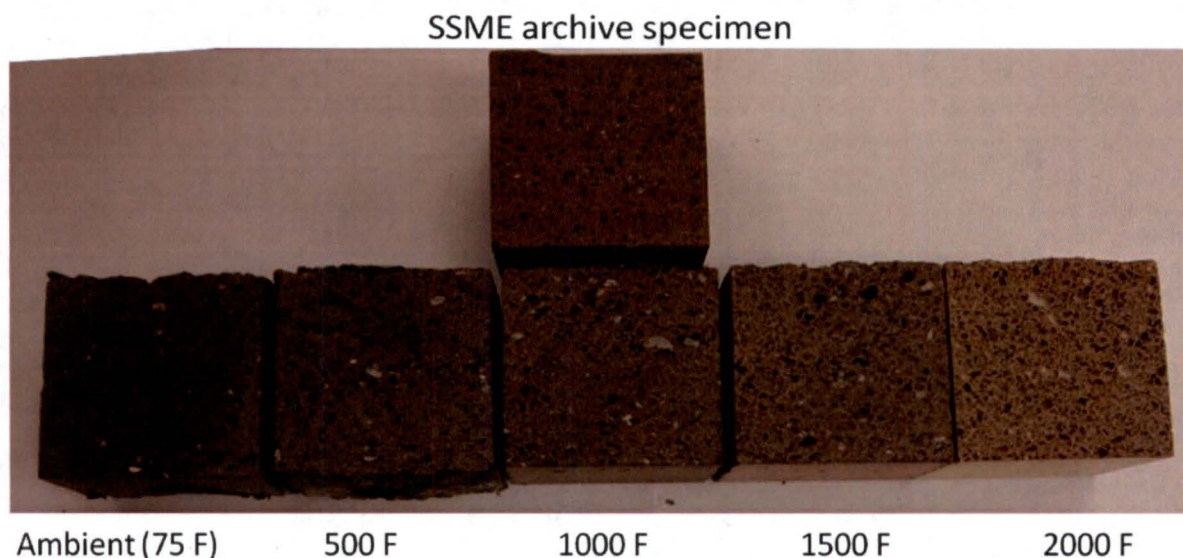


Figure 7. Array of heat-treated FF specimens (100% water content)

4.2 Crushing Strength

The average compression strengths for each condition are displayed in Figure 8. Raw data [8] for each sample is listed in Appendix D. Crushing strength data [8]. An apparent and expected result of the heat treatment was the decrease in crushing strength. The application of heat to the FF

cubes causes dehydration, resulting in a decrease in the size of the molecules involved in the cement bonds. This results in decreasing compressive strength of the material, as well as increasing the porosity. At high temperatures, the material will sinter resulting in an increase in crushing strength and decrease in porosity. The sintering temperature for FF was not reached in this experiment and must be greater than 2000°F.

Subsequent statistical analyses (two-way ANOVA) of the data at a 95% confidence level indicate that both water content and heat treatment factor significantly into the crushing strength of the refractory material. Figure 9 summarizes the statistical results from those responses with respect to heat treatments. Minitab results for the same responses with respect to water content are tabulated in Appendix A, Minitab Outputs. Without considering water content, the crushing strengths for heat treatment sample sets that are statistically differentiable are at 75°F (ambient), 1000°F, and 2000°F. Crushing strengths at treatments 500°F and 1000°F are statistically indistinguishable, and the crushing strength range for treatment 1500°F is indistinguishable from every treatment except 75°F.

Water content was found to have an effect on crushing strength only for ambient curing and a heat treatment of 500°F. At higher temperature heat treatments, water content became an indistinguishable factor in crushing strengths. These results are rigorously observable in the Minitab outputs in Appendix A (Figure 15 - Figure 19). For ambient cured samples, the strongest were those made with the manufacturer recommended amount of water. It is generally thought that the higher the water content the lower the crushing strength. This held true for the high water content samples, as they had the lowest crushing strength. The low water content samples had a crushing strength between the other two. The low water content mix was the most difficult to cast and it did not flow very well into the molds. It is unclear if the lack of strength is due to incomplete hydration of the cement, or due to poor flow properties.

Figure 10 shows crushing strength of the cast ambient cured specimens prepared in this study with the gunned specimens prepared previously [3]. The gunned specimens have crushing strength similar to the cast specimens with non-ideal water content.

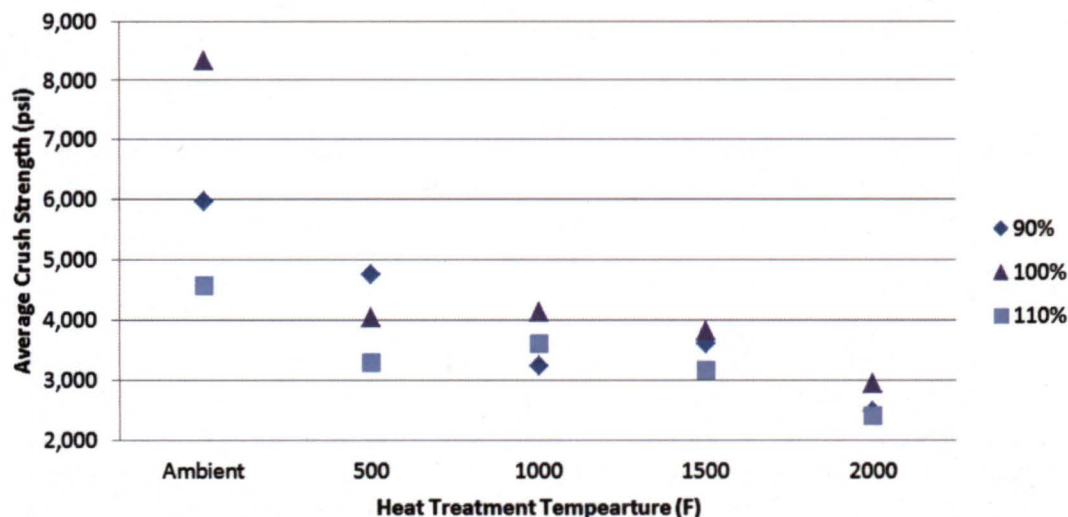


Figure 8. Crush strength results FF: Various water compositions and heat treatments

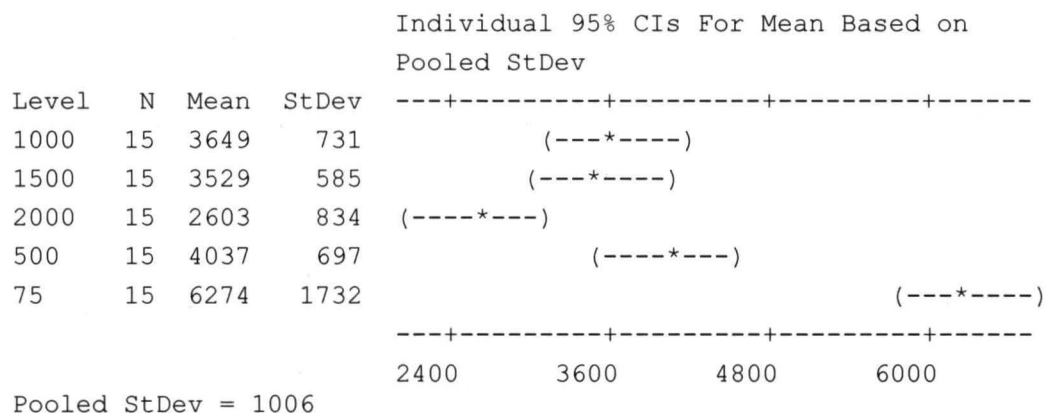


Figure 9. Minitab output: One-way ANOVA: Crush strength (psi) versus heat Trt (°F)

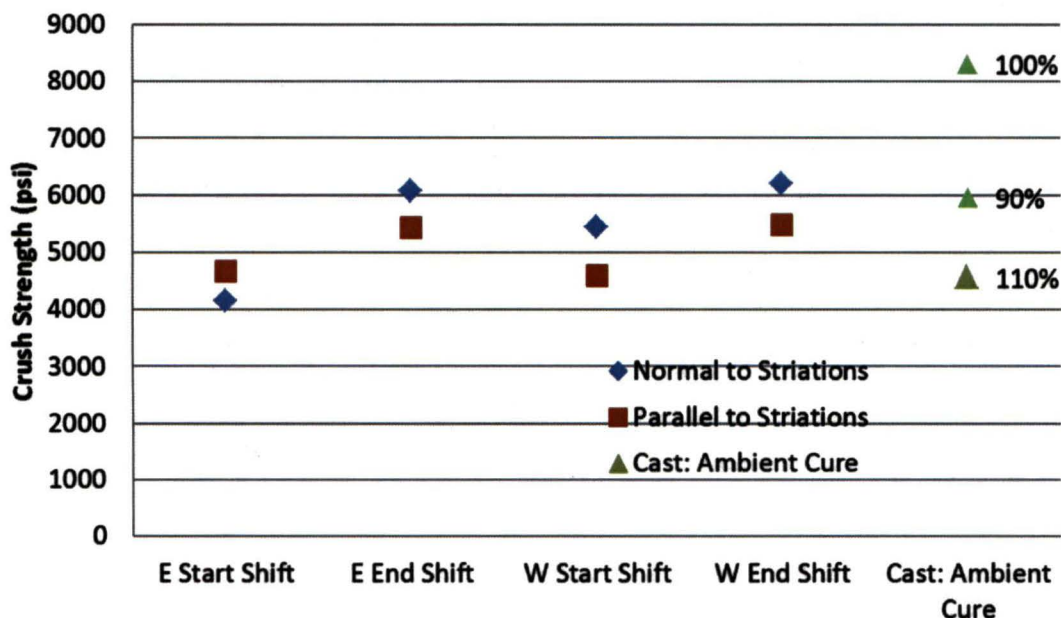


Figure 10. Comparison of crushing strength between gunned specimens [3] and cast specimens prepared in this study

4.3 Porosity and Bulk Density

Porosity is the ratio of the volume of the open pores to the bulk volume of a material, expressed as a percentage. Bulk density is defined as the mass of many particles of a material divided by the total volume they occupy. The total volume includes particle volume, inter-particle void volume and internal pore volume. Bulk density is not an intrinsic property of a material and it can change depending on how the material is handled. As with crushing strength, both water content and heat treatments factor significantly into apparent porosity and bulk density of the refractory material. Figure 11 and **Error! Reference source not found.** show the averages of

porosity and bulk density for all conditions. Complete data used to calculate porosity and bulk data are listed in Appendix E. Figure 11 shows the statistical results for porosity with respect to heat treatments. Minitab results for the same responses with respect to water content are tabulated in Appendix A (Figure 20 - Figure 24).

Porosity increases with higher heat treatments. Three distinct porosity ranges are apparent at heat treatments 75°F, 500°F, and 1000-2000°F, as 1000°F, 1500°F, and 2000°F produce statistically indistinguishable porosity differences.

Water content affected apparent porosity on ambient and 500°F treated samples, but was an insignificant factor for heat treatments exceeding 1000°F. This suggests that water content will become less important as the material ages and is exposed to heat from rocket exhaust. These results are rigorously observable in the Minitab outputs in Appendix A.

The bulk density decreases with increasing heat treatment, as shown in **Error! Reference source not found.** A two way ANOVA showed that both water content and heat treatment were significant factors in bulk density. Bulk density was affected by heat treatment for all water contents. For the 100 and 110% water contents, bulk density was significantly different at all heat treatments except 1500 and 2000°F. For the 90% water content samples, the ambient and 500°F heat treatments were distinguishable, but the 1000, 1500 and 2000°F were not distinguishable from each other. As the heat treatment temperature is increased, the bulk density should decrease as the material dehydrates.

Table 2 lists the average porosity and bulk density of cast ambient cured samples and that of a historic sample taken from the SSME flame deflector. Statistical analysis indicated that the porosity of the SSME samples were significantly different from only the cast specimen with 110% water content. The bulk density of the SSME samples was found statistically to be greater than that of the 100 and 110% water content samples. There was no statistical difference between the SSME and 90% water content samples.

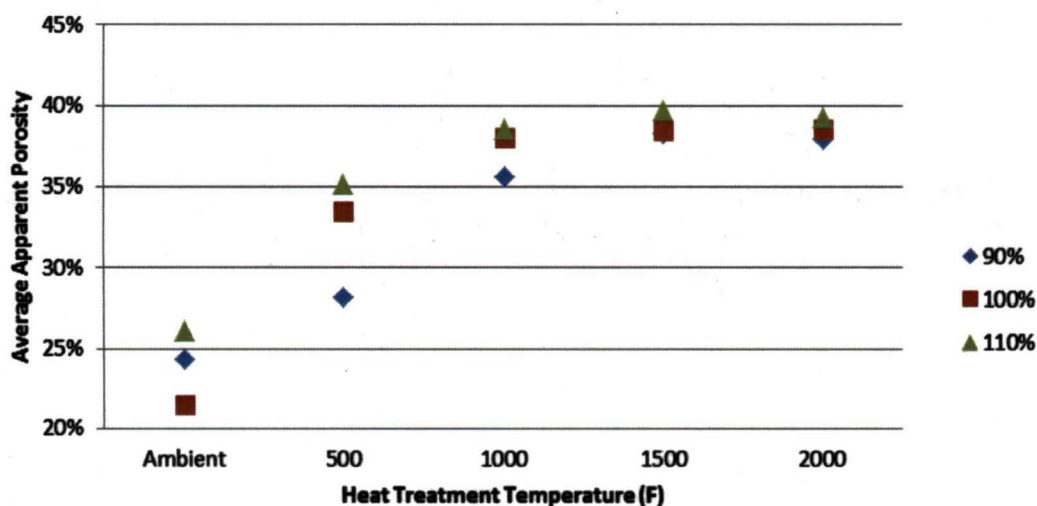


Figure 11. Apparent porosity of FF with different water contents and heat treatments

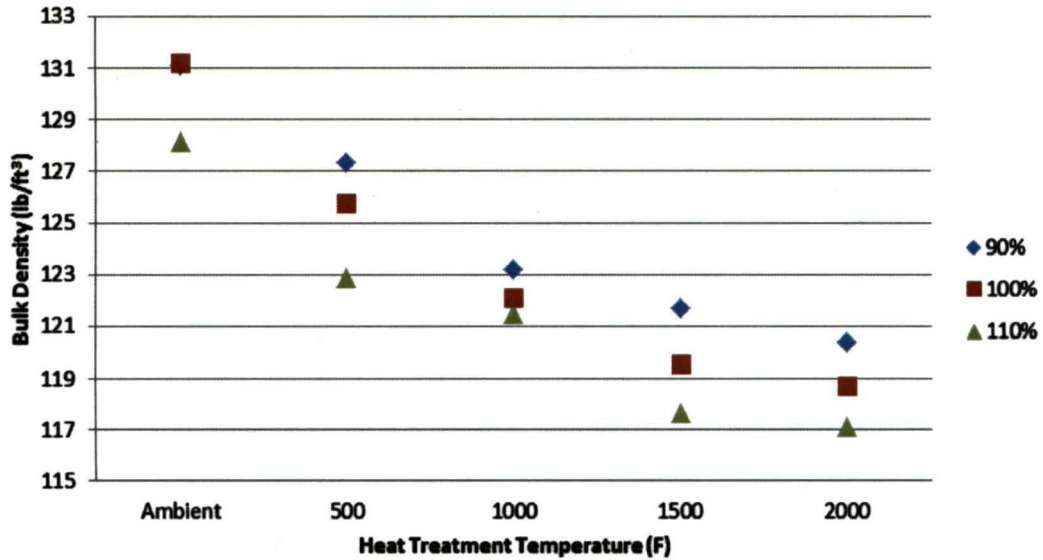


Figure 12. Bulk density of FF with different water contents and heat treatments

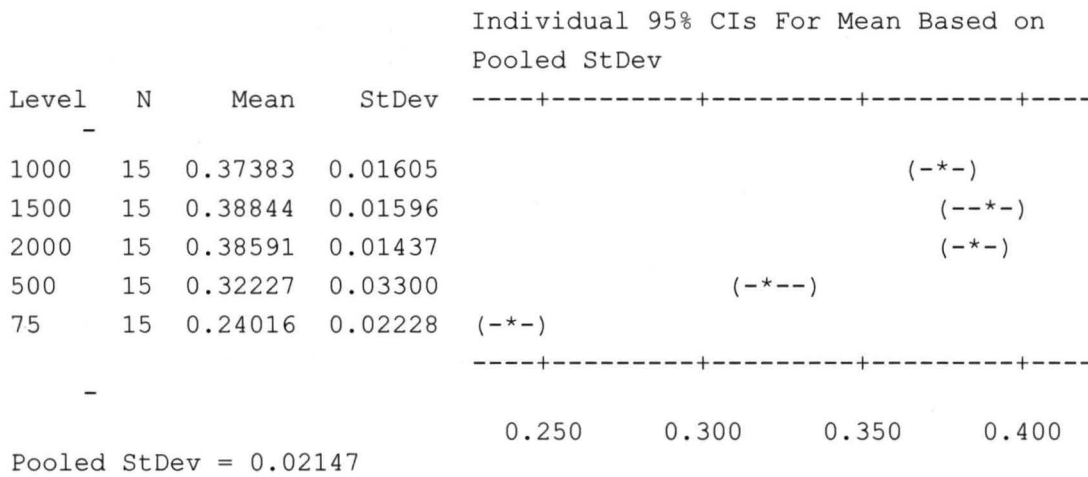


Figure 13. Minitab output: One-way ANOVA: Apparent Porosity versus Heat Treatment (°F)

Table 2. Comparison of apparent porosity and bulk density of cast samples and historic samples from SSME flame deflector

	Apparent Porosity (%)	Bulk Density (lbs/ft ³)
SSME	22.6	134.35
90% water content – 75 °F	24.3	131.11
100% water content – 75 °F	21.5	131.23
110% water content – 75 °F	26.2	128.15

4.4 SEM Analysis

SEM analysis of low, midrange, and high heat treatments indicate a characteristic variation in surface structure, regardless of specimen water composition. Figure 12 displays these surface structures for 100% water content FF. The most distinct surface feature is present for 2000°F heat treatments. Each of the water contents presents these coral-like features consistently throughout the fractured surfaces, as well as in the powder (see Figure 24 in Appendix A for side-by-side of 2000°F-treated water content specimens). Similarly, for 1000 °F treatments, every specimen contains feathered features, although the frequencies vary (see Figure 23 in Appendix A for side-by-side of 1000°F-treated water content specimens). The surface structure at ambient cures is consistent among specimens in its relative amorphous and “crumbly” appearance (see Figure 25 in Appendix A for side-by-side of 75°F-treated water content specimens). However, identical structures are difficult to distinguish, even within a single specimen. These visual results support the analytical results that indicate the insignificance of water content on strength or porosity for cures exceeding 1000°F.

Additionally, SEM images reveal unreacted crystal structures, as apparent in each heat treatment for 90% water content specimens (see Figure 26 in Appendix A). These unreacted crystals were determined via elemental analysis (EDS) to be calcium oxide, which undergoes hydration reactions to contribute to bonding in the cement and strength of the refractory. The observation of CaO in unbound form indicates the lack of water available in the 90% FF specimens to complete hydration bonding. Similar crystalline structures were not observed in either 100%- or 110%- water content specimens.

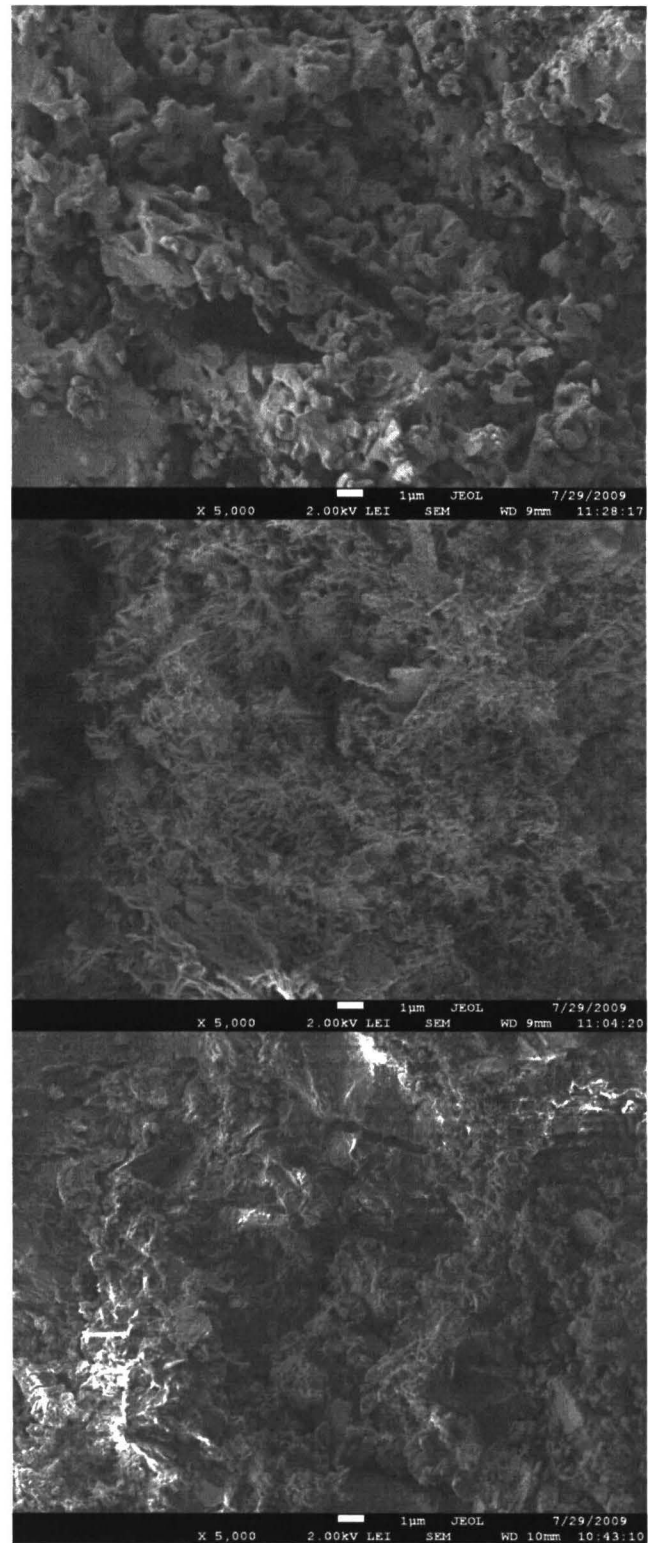


Figure 14. From top to bottom, 5000x SEM images of 100% FF treated at 2000°F, 1000°F, and 75°F

5 CONCLUSIONS

The conclusions are summarized as follows:

- Water content and heat treatment are significant factors in the performance of FF.
- In general, crushing strength and bulk density decrease while porosity increases with increasing heat treatment temperatures.
- Water content has a statistically significant effect on the properties of FF at curing temperatures below 500°F. After higher heat treatments, it is not an important factor.
- The optimum water content resulted in the strongest samples for ambient curing. There was speculation that decreasing water content would increase strength, but this was not the case. It is not clear if the decrease in strength for the low water content specimens is due to water content or poor flow properties of the material.
- SEM analysis can be used to observe the effects of different conditions such as water contents and heat treatments on the material, by allowing the identification of different phases and structures in the material. Its use as a quick assessment method is promising, pending further rigorous evaluation.
- New materials would show improvement if they were less affected by water content or temperatures.

6 REFERENCES

1. David Trejo and Associates, *Prefabricated Refractory Panels for use in KSC's Flame Deflectors: A Feasibility Study*. 2009.
2. Luz Marina Calle, David Trejo, and Justin Rutkowsky, *NASA/TM-2006-214197 Evaluation of Alternative Refractory Materials for the Main Flame Deflectors at KSC Launch Complexes*. 2006.
3. NASA Malfunction Analysis, *KSC-MSL-2008-0401: Fondy Fyre WA-1G Modulus of Rupture and Cold Crushing Strength Tests*. 2008.
4. ASTM International, *C133 - 97 Standard Test Methods for Cold Crushing Strength and Modulus of Rupture of Refractories*. 2008.
5. ASTM International, *C20 - Standard Test Methods for Apparent Porosity, Water Absorption, Apparent Specific Gravity, and Bulk Density of Burned Refractory Brick and Shapes by Boiling Water*. 2005.
6. ASTM International, *C862 - 02 Standard Practice for Preparing Refractory Concrete Specimens by Casting*. 2008.
7. Pryor Giggey Co., *Special Mixing/Using Instructions for Fondy Fyre (R) WA-1*.
8. NASA Malfunction Analysis, *KSC-MSL-2009-0209: Study the properties of refractory concrete for the LC-39 Flame Deflectors*. 2009.

APPENDIX A. MINITAB OUTPUTS

Overlapping confidence intervals around the means displayed below indicate a lack of statistically significant differences among sample sets.

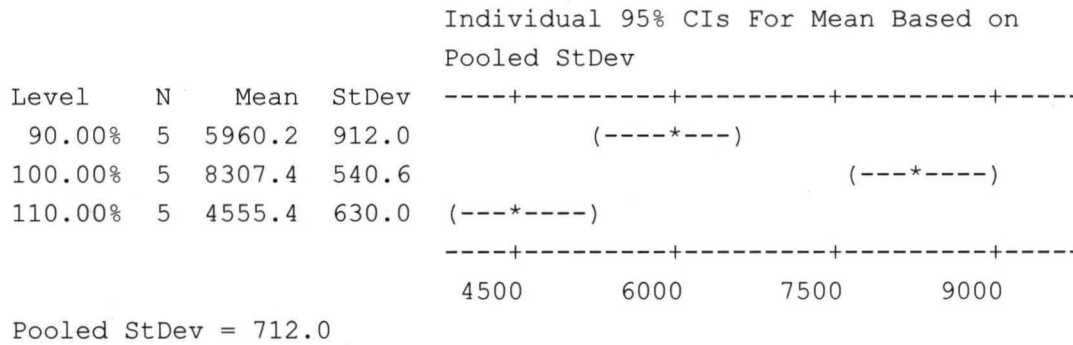


Figure 15. One-way ANOVA: 75°F Crush strength versus Water Composition

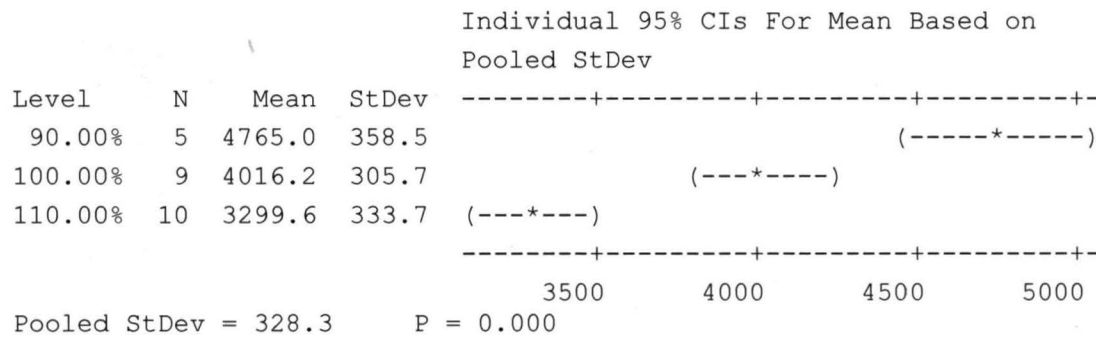


Figure 16. One-way ANOVA: 500°F Crush strength versus Water Composition

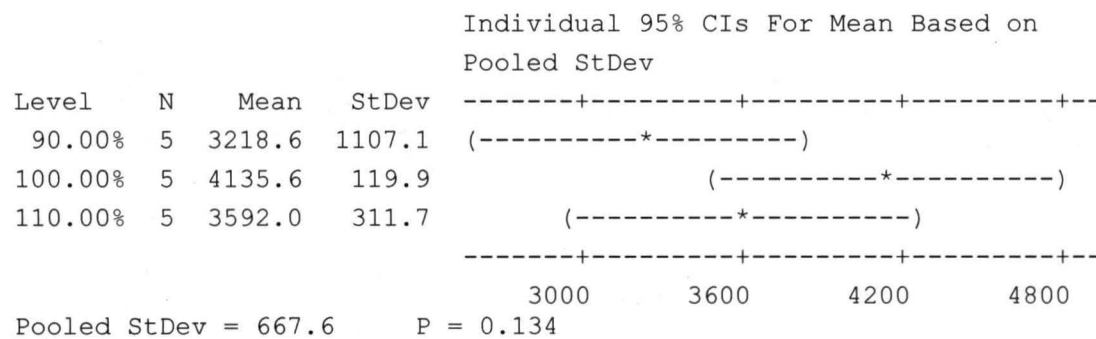


Figure 17. One-way ANOVA: 1000°F Crush strength versus Water Composition

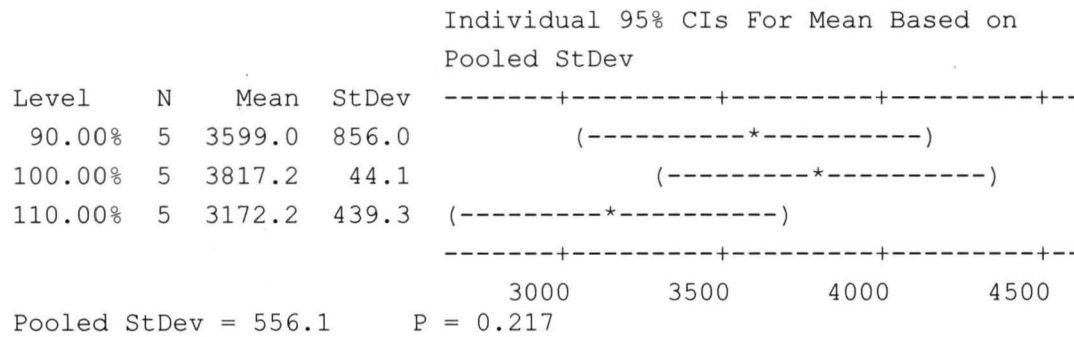


Figure 18. One-way ANOVA: 1500°F Crush strength versus Water Composition

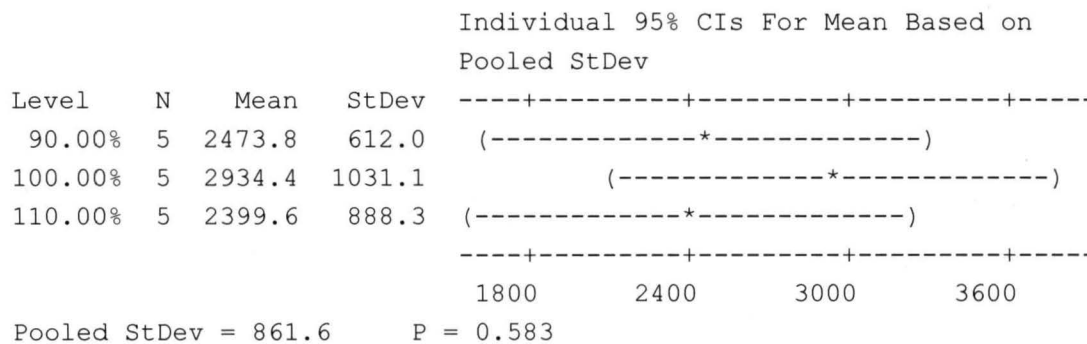


Figure 19. One-way ANOVA: 2000°F Crush strength versus Water Composition

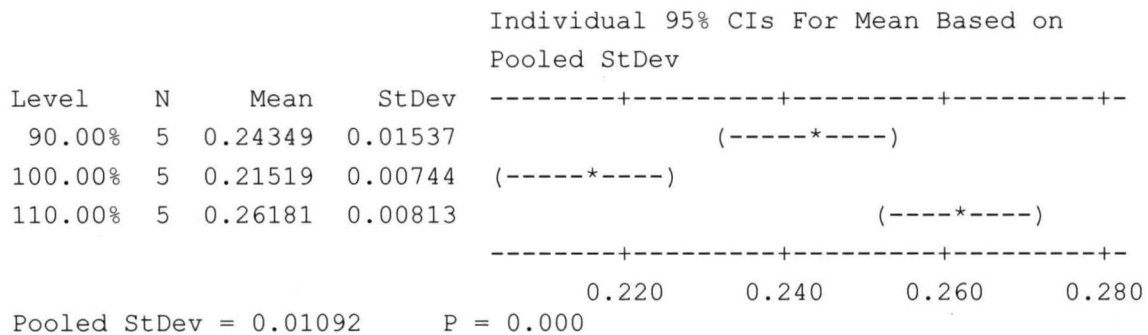


Figure 20. One-way ANOVA: 75°F Porosity versus Water Composition

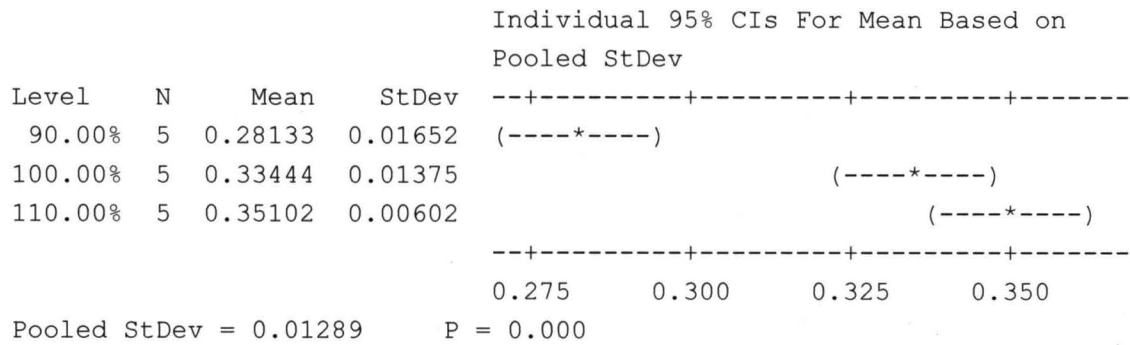


Figure 21. One-way ANOVA: 500°F Porosity versus Water Composition

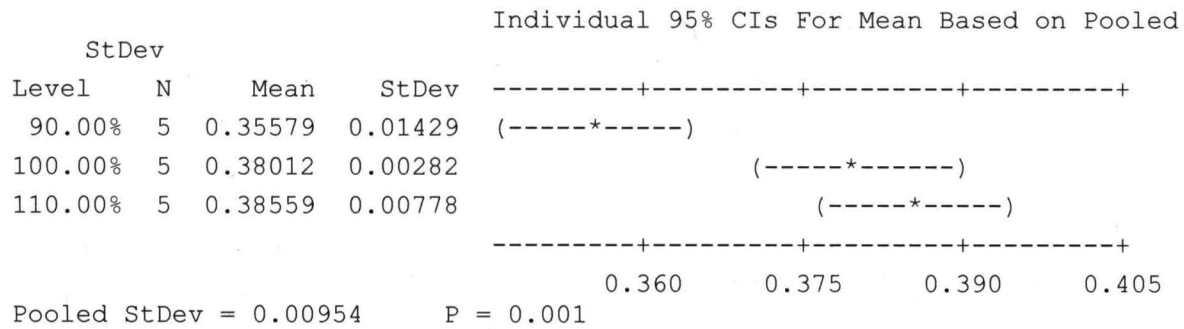


Figure 22. One-way ANOVA: 1000°F Porosity versus Water Composition

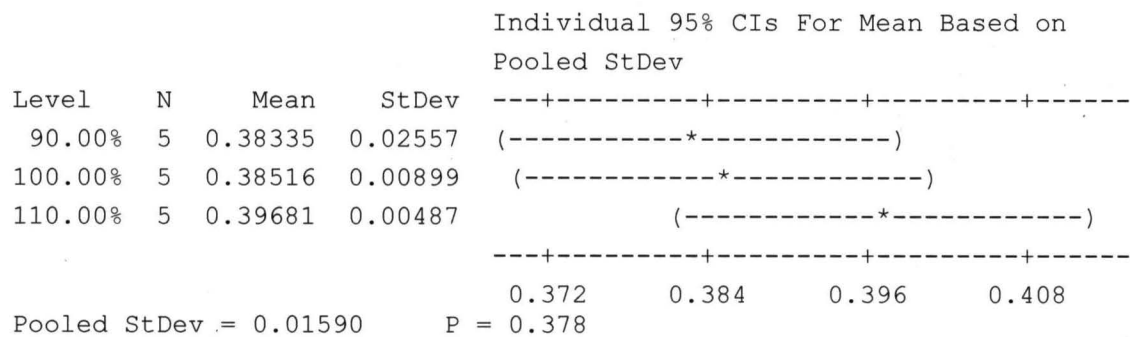


Figure 23. One-way ANOVA: 1500°F Porosity versus Water Composition

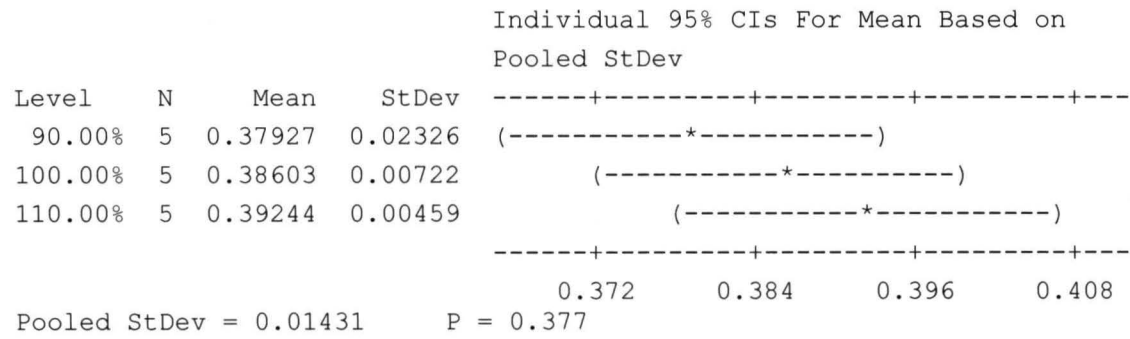


Figure 24. One-way ANOVA: 2000°F Porosity versus Water Composition

APPENDIX B. ADDITIONAL SEM IMAGES

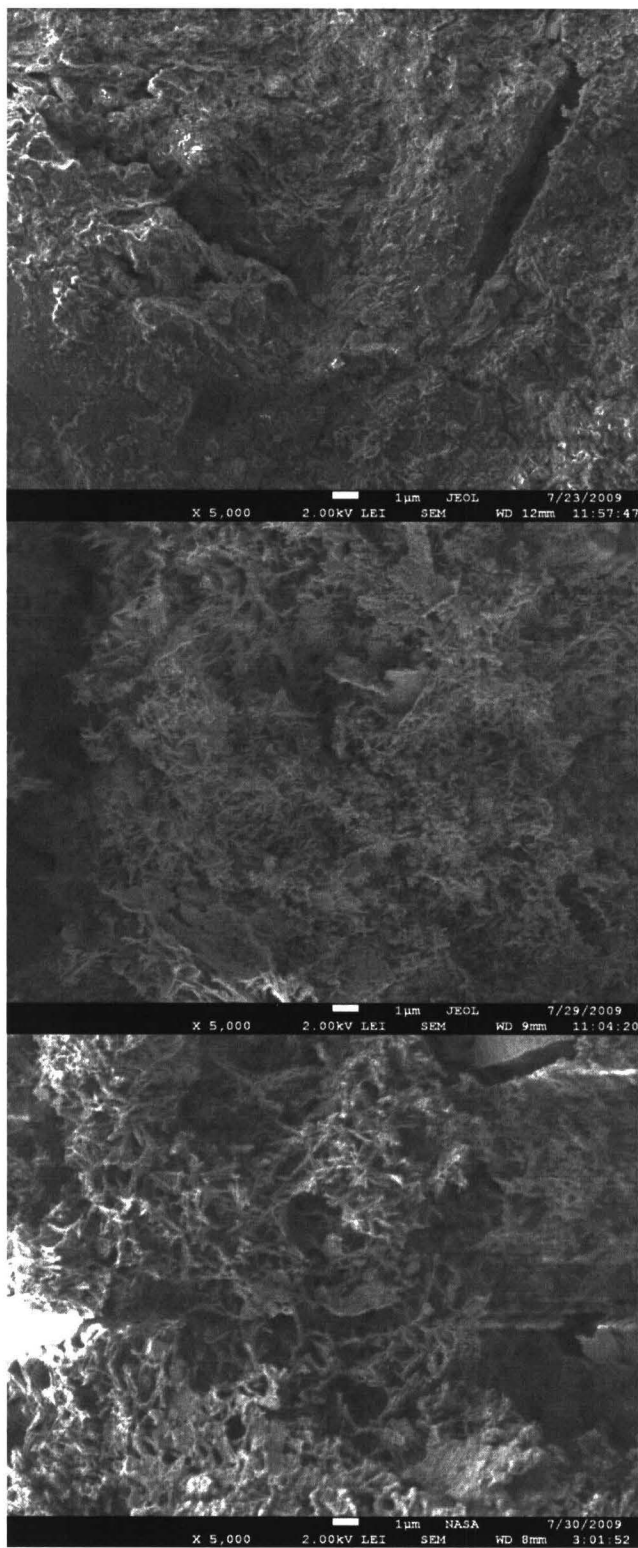


Figure 25. From top to bottom: 5000x SEM images of 1000°F heat treatment for 90%, 100%, and 110% water content FF

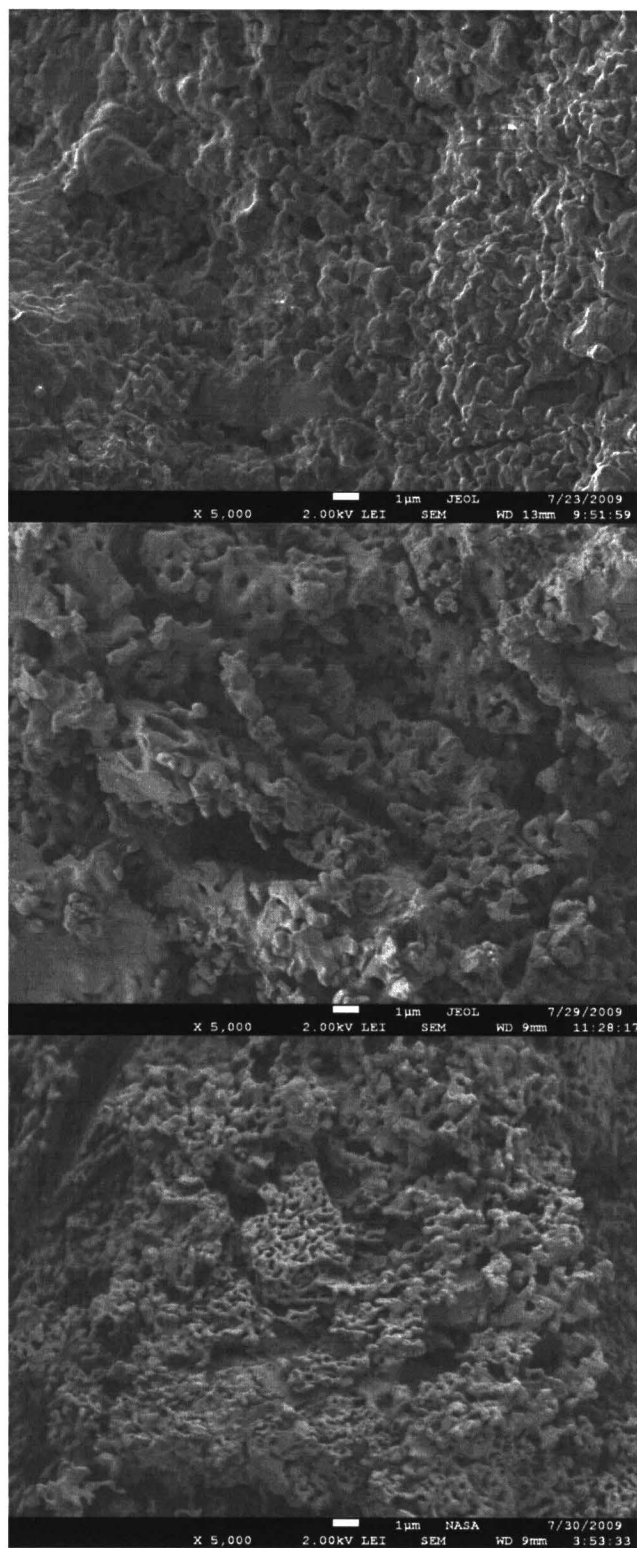


Figure 26. From top to bottom: 5000x SEM images of 2000°F heat treatment for 90%, 100%, and 110% water content FF

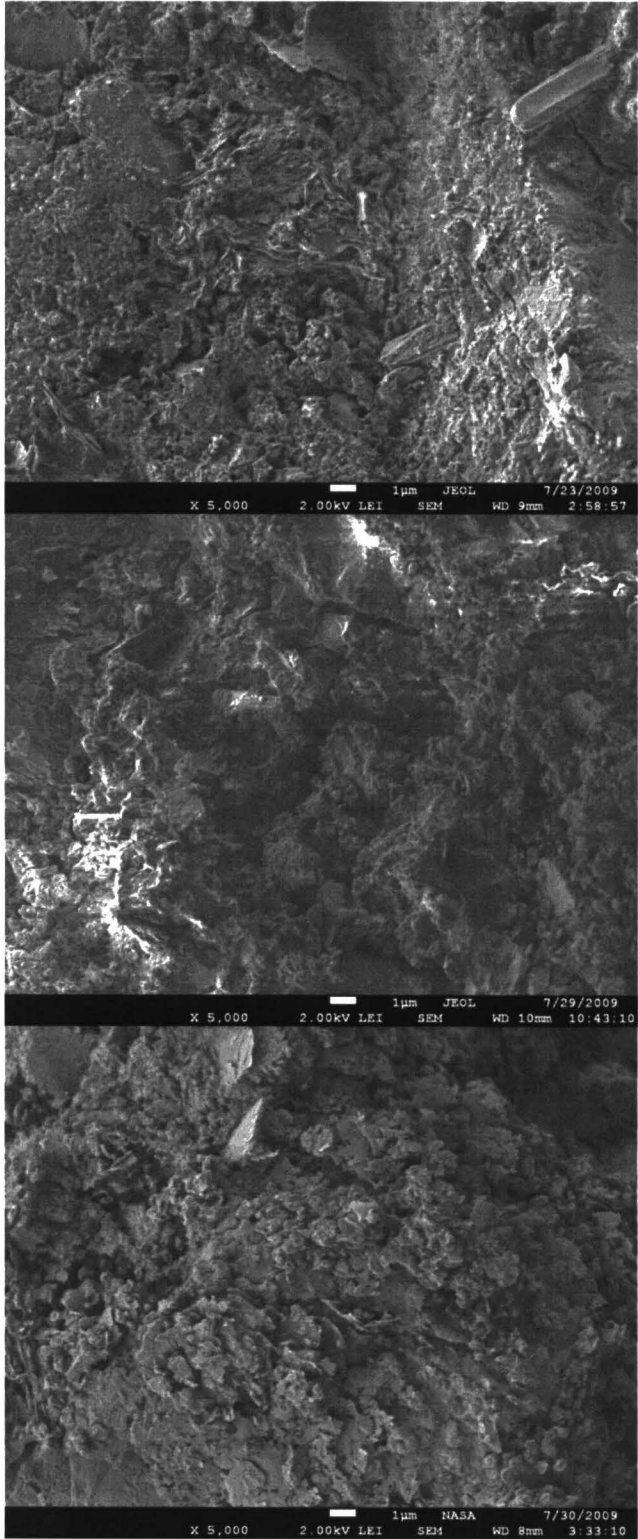


Figure 27. From top to bottom: 5000x SEM images of 75°F heat treatment for 90%, 100%, and 110% water content FF

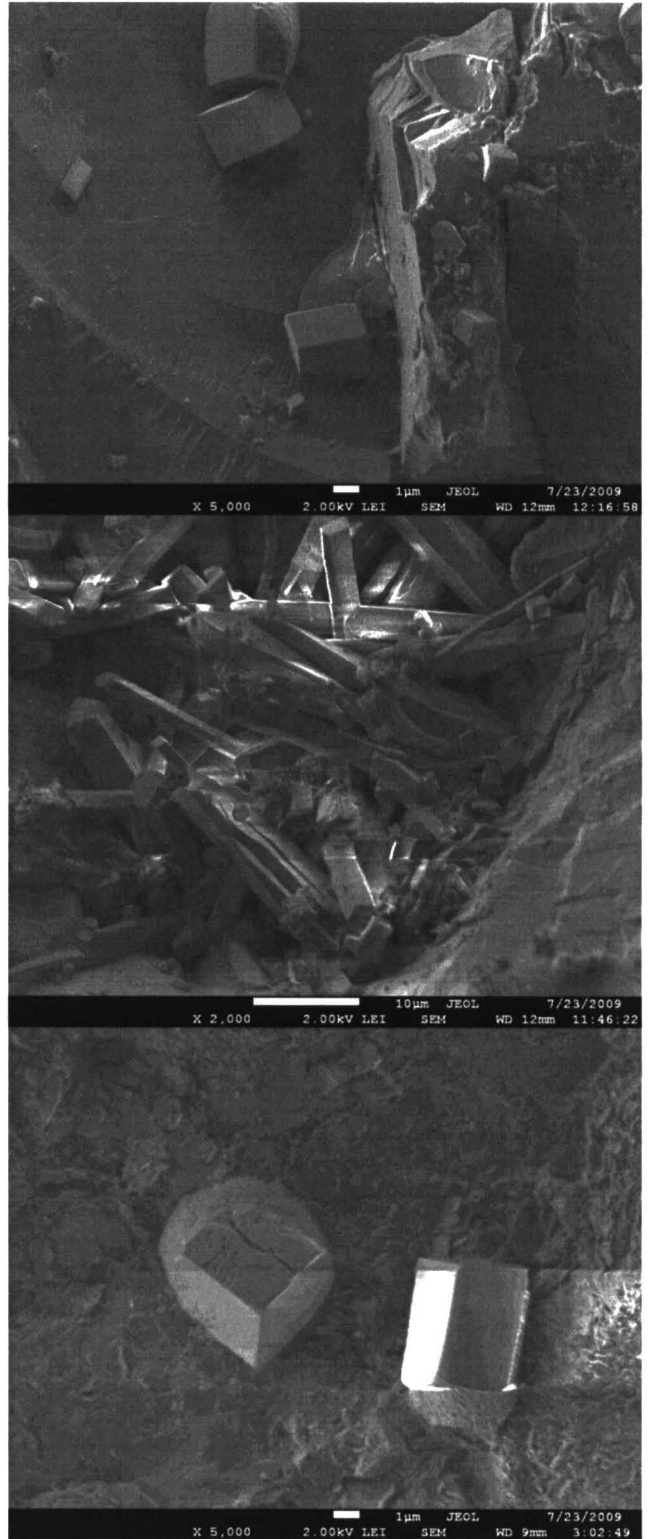


Figure 28. From top to bottom: SEM images of 90% water content heat treated to 1000°F, 1000°F and 75°F

APPENDIX C. SPECIAL MIXING/USING INSTRUCTION
FONDU FYRE® WA-1



Special Mixing/Using Instructions
FONDU FYRE® WA-1

NOTE: These notes are to be considered addenda to the Fondu Fyre Casting Procedures and are written specifically for the LC-39A SRB side flame deflector repair, November 2007.

EQUIPMENT: Use a 15-20 ft³ paddle mixer; do not use a rotary drum style concrete mixer. Mixer must be clean and free of any Portland cement residue.

MIXING: Dry mix material for one minute or less and then add the smallest amount of water necessary to achieve the flow for the given geometry. The water required is typically 14% by weight. The proper consistency is initially determined by the ball-in-hand test. Adjustments to the water may be necessary throughout the casting process as variations are common.

FORMS: Forms should be steel plate (preferred) or double staggered 1/2" plywood. Plywood forms must be reinforced with walers and held together by all-thread. Forms must be water proofed before casting.

The forms should be laid flush on the existing refractory and sealed using silicone or caulk. Forms should be secured to the existing refractory using "red heads." Peek holes every six inches vertically and 12 inches horizontally must be drilled in the forms to ensure proper castable consolidation. As the castable fills inside the forms and the begins to flow out of the holes, the holes must be plugged.

If an area larger than 6 feet in either direction needs to be patched, the area must be sectioned into smaller areas with alternating sections poured on consecutive days (i.e. in a checker board fashion).

SURFACE PREPARATION:

The surface of the existing refractory should be left as rough as possible with all loose material and dust removed.

Do not use bonding agent on the existing refractory, as experience has shown this may actually prevent bonding between new and existing refractory.

Dampen the existing refractory slightly before casting.

CASTING:

Use 2" probe vibrators inside the forms to flow the material. Vibrators must be clean and free of Portland cement residue.

As the form is filled the top of the form should be capped off at the refractory surface. An angled chute will facilitate pouring the refractory into the hole and a board or plate can be slid in as the chute is filled.

Do not remove forms for 24 hours. A small sample can be poured during casting as a set time indicator. Caution should be taken as open refractory will set faster than refractory enclosed in a form.

Important:

The following factors will adversely affect the density, strength, and setting properties of this castable:

- A) Admixtures
- B) Dirty/Hot water
- C) Dirty Mixer
- D) Excessive Water
- E) Over Mixing
- F) Excessive Vibration
- G) Gunning or Pumping

APPENDIX D. CRUSHING STRENGTH DATA [8]

	Specimen label	Width (in)	Thickness (in)	Maximum load (lbf)	Compressive stress (psi)
1	090%-0075F-01	2.01	2.04	25395	6193
2	090%-0075F-02	2.00	2.04	21474	5250
3	090%-0075F-03	2.00	2.04	25483	6246
4	090%-0075F-04	2.01	2.01	29135	7211
5	090%-0075F-05	2.01	2.01	19802	4901
6	100%-0075F-06	2.02	2.02	36121	8852
7	100%-0075F-07	2.01	2.03	32798	8038
8	100%-0075F-08	2.00	2.04	36147	8881
9	100%-0075F-09	2.02	2.03	33287	8118
10	100%-0075F-10	2.00	2.01	30743	7648
11	110%-0075F-11	2.00	2.03	20666	5090
12	110%-0075F-12	2.00	2.00	18860	4715
13	110%-0075F-13	2.00	2.01	20769	5154
14	110%-0075F-14	2.00	2.03	15048	3706
15	110%-0075F-15	1.98	2.00	16282	4112
16	090%-0500F-16	2.03	2.03	19807	4806
17	090%-0500F-17	2.02	2.03	21005	5110
18	090%-0500F-18	2.02	2.00	17846	4406
19	090%-0500F-19	1.98	2.00	17377	4388
20	090%-0500F-20	2.00	1.98	20257	5115
21	100%-0500F-21	2.00	2.00	17271	4318
22	100%-0500F-22	1.99	2.04	14328	3521
23	100%-0500F-23	2.00	2.05	16240	3961
24	100%-0500F-24	1.99	2.02	17014	4222
25	100%-0500F-25	2.06	2.00	17305	4210
26	110%-0500F-26	1.99	2.10	15772	3774
27	110%-0500F-27	2.02	2.06	12838	3093
28	110%-0500F-28	2.01	2.01	11559	2861
29	110%-0500F-29	2.01	2.01	13211	3270
30	110%-0500F-30	2.01	2.04	14387	3500
31	090%-1000F-31	2.02	2.00	19792	4887
32	090%-1000F-32	2.00	2.00	10182	2545
33	090%-1000F-33	1.99	2.00	14217	3563
34	090%-1000F-34	2.00	2.04	8054	1979
35	090%-1000F-35	2.00	2.06	12849	3119
36	100%-1000F-36	2.00	2.00	16418	4094
37	100%-1000F-37	2.00	2.01	17291	4290
38	100%-1000F-38	1.99	2.02	16932	4212
39	100%-1000F-39	2.00	2.03	16187	3977
40	100%-1000F-40	2.00	2.01	16502	4105

	Specimen label	Width (in)	Thickness (in)	Maximum load (lbf)	Compressive stress (psi)
41	110%-1000F-41	2.00	2.02	14929	3704
42	110%-1000F-42	2.00	2.04	14818	3641
43	110%-1000F-43	1.99	2.01	13380	3345
44	110%-1000F-44	1.99	2.04	16391	4028
45	110%-1000F-45	1.99	2.02	13032	3242
46	090%-1500F-46	1.99	2.00	12031	3023
47	090%-1500F-47	2.00	2.02	11894	2951
48	090%-1500F-48	2.01	2.01	17821	4411
49	090%-1500F-49	2.03	2.00	12010	2958
50	090%-1500F-50	2.06	2.00	19214	4652
51	100%-1500F-51	1.98	2.04	15193	3771
52	100%-1500F-52	1.99	2.00	15382	3865
53	100%-1500F-53	2.02	1.99	15153	3770
54	100%-1500F-54	2.04	1.99	15562	3833
55	100%-1500F-55	2.00	2.02	15542	3847
56	110%-1500F-56	1.98	2.01	11459	2887
57	110%-1500F-57	1.98	1.99	10276	2608
58	110%-1500F-58	1.99	2.00	14926	3750
59	110%-1500F-59	2.00	2.02	13473	3335
60	110%-1500F-60	2.00	2.06	13519	3281
61	090%-2000F-61	2.01	2.01	7388	1829
62	090%-2000F-62	2.00	2.02	11003	2730
63	090%-2000F-63	2.00	2.02	13742	3393
64	090%-2000F-64	1.98	2.01	9285	2333
65	090%-2000F-65	1.99	2.00	8296	2084
66	100%-2000F-66	2.02	2.04	9767	2370
67	100%-2000F-67	2.02	2.04	19175	4676
68	100%-2000F-68	1.99	2.02	8652	2152
69	100%-2000F-69	2.00	2.03	9795	2412
70	100%-2000F-70	2.02	2.06	12742	3062
71	110%-2000F-71	1.96	2.02	7531	1912
72	110%-2000F-72	2.05	2.02	7810	1886
73	110%-2000F-73	2.08	2.04	10984	2595
74	110%-2000F-74	1.96	2.00	15146	3873
75	110%-2000F-75	2.01	2.00	6945	1732

APPENDIX E. DATA USED TO CALCULATE POROSITY AND BULK DENSITY ACCORDING TO ASTM C20

<i>Water Content</i>	<i>Heat treatment</i>	<i>Dry Mass (g)</i>	<i>Saturated Mass (g)</i>	<i>Suspended Mass (g)</i>
90%	75 °F	278.04	311.37	178.3
90%	75 °F	267.76	295.74	169.6
90%	75 °F	269.71	300.97	174.5
90%	75 °F	285.49	316.67	184.4
90%	75 °F	266.86	301.51	169.4
100%	75 °F	278.44	306.86	174.7
100%	75 °F	281.66	309.98	174.9
100%	75 °F	275.4	304.96	174.6
100%	75 °F	282.19	310.02	176.1
100%	75 °F	279.41	307.96	176.2
110%	75 °F	263.96	298.03	169.1
110%	75 °F	278.16	313.81	178.8
110%	75 °F	271.3	304.74	173.5
110%	75 °F	261.51	296.7	167.8
110%	75 °F	278.9	312.79	178.8
90%	500 °F	254.61	290.34	165.3
90%	500 °F	275.66	309.97	176.6
90%	500 °F	249.18	286.57	162.4
90%	500 °F	275.64	312.14	179
90%	500 °F	267.9	305.75	174.5
100%	500 °F	263.48	305.7	175
100%	500 °F	258.77	302.51	176
100%	500 °F	266.87	313.76	179.2
100%	500 °F	260.35	304.31	174.1
100%	500 °F	264.01	304.88	176.1
110%	500 °F	256.64	303.23	172.2
110%	500 °F	258.55	303.41	174
110%	500 °F	264.96	310.39	177.8
110%	500 °F	256.4	303.02	171.5
110%	500 °F	257.52	304.31	172.8
90%	1000 °F	255	297.32	171.3
90%	1000 °F	250.88	298.97	169.2
90%	1000 °F	254.31	301.07	171.4
90%	1000 °F	249.51	296.32	168.2
90%	1000 °F	258.84	303.15	175.3
100%	1000 °F	254.3	304.41	174

<i>Water Content</i>	<i>Heat treatment</i>	<i>Dry Mass (g)</i>	<i>Saturated Mass (g)</i>	<i>Suspended Mass (g)</i>
100%	1000 °F	259.89	309.75	177.7
100%	1000 °F	259.94	309.81	177.7
100%	1000 °F	257.89	307.95	176.2
100%	1000 °F	256.58	306.55	175.5
110%	1000 °F	257.1	308.34	176
110%	1000 °F	258.92	312.21	176.9
110%	1000 °F	257.42	306.03	176.6
110%	1000 °F	249.68	300.46	170.8
110%	1000 °F	259.78	309.66	178.3
90%	1500 °F	265.64	315.02	182
90%	1500 °F	260.24	308.68	177.8
90%	1500 °F	244.11	296.73	167.1
90%	1500 °F	241.45	294.67	166.3
90%	1500 °F	266.07	312.82	181.1
100%	1500 °F	255.94	304.27	173.9
100%	1500 °F	255.15	305.54	173.8
100%	1500 °F	251.02	303.01	170.4
100%	1500 °F	248.71	299.18	169.2
100%	1500 °F	247.46	298.68	168.1
110%	1500 °F	254.68	307.74	173.3
110%	1500 °F	256.66	309.58	174.5
110%	1500 °F	248.47	300.27	169.3
110%	1500 °F	219.45	267.15	149.3
110%	1500 °F	255.86	309.7	174.2
90%	2000 °F	260.19	309.44	176.8
90%	2000 °F	264.51	312.28	178
90%	2000 °F	264.68	313.79	179.7
90%	2000 °F	239.83	294.01	163.6
90%	2000 °F	261.04	313.78	177.7
100%	2000 °F	245.48	295.55	164.5
100%	2000 °F	254.36	304.17	172.9
100%	2000 °F	253.96	304.75	173.3
100%	2000 °F	252.44	303.3	170.9
100%	2000 °F	245.97	298.07	167.2
110%	2000 °F	249.64	302.67	168.5
110%	2000 °F	261.87	315.56	177.2
110%	2000 °F	254.65	306.29	172.8
110%	2000 °F	259.14	313.85	175.7
110%	2000 °F	253.24	307.17	171